THE JOURNAL OF PHYSICAL CHEMISTRY C

Article

Cite This: J. Phys. Chem. C 2019, 123, 3657−3663

pubs.acs.org/JPCC

Tunneling Diffusion of Excess Protons in Amorphous Solid Water at 10 and 80 K

Du Hyeong Lee, Hani Kang, and Heon Kang*

Department of Chemistry, Seoul National University, 1 Gwanak-ro, Seoul 08826, Republic of Korea

ABSTRACT: This work explores the plausibility of quantum tunneling of excess protons in amorphous solid water (ASW) at temperatures as low as 10 K. The transport of protons from a proton donor (HCl) to an acceptor (NH_3) species located at a controlled separation distance in an ASW film was investigated at 10 and 80 K. The proton transfer efficiency was measured by quantitation of the yield of ammonium ions using reflection−absorption infrared spectroscopy. The average transport distance of excess protons in the ASW films was ∼10 water molecules in the temperature range 10−80 K and showed no noticeable dependence on the temperature. On the other hand, the transport of protons along the surface of the ASW film was restricted to within a range of two water molecules at 10 K because of an energy barrier. The mobility of excess protons in the interior of ASW at temperatures close to 10 K indicated quantum tunneling of protons, most likely in the microscopic crystalline regions of the ASW samples.

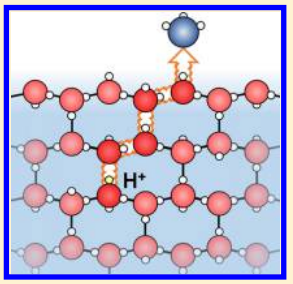

1. INTRODUCTION

The mobility of excess protons (positive protonic defects) in ice is intimately related to the diverse physical[1,2] and chemical properties of ice.[3] The general concept of proton transport in ice was originally formulated by Jaccard[4,5] and Onsager[6] and is now well accepted through extensive experimental verification.[7−23] The excess protons in ice move along its hydrogen-bonded network via an efficient hopping relay (Grotthuss) mechanism.[1,2] The proton passage along the hydrogen-bonded water chain polarizes the direction of the hydrogen bonds, which blocks the passage of the subsequent protons hopping along the same path. Therefore, for a continuous flow of protons, reorientation of water molecules (Bjerrum defect motion) must take place to depolarize the hydrogen-bond direction. As water reorientation in ice is activated at temperatures above 130 K,[9−11] an ice crystal can be an effective protonic conductor only at a high temperature. Acceptance of this elegant mechanism of proton transport in ice in the scientific community, however, was not a straightforward process, and there were opposing arguments and confusions, which have been briefly summarized by Devlin.[23] The concept of proton mobility in the ice interior was challenged by the report that H_3O^+ ions that were soft-landed on an ice film surface remained on the surface over a wide temperature range,[24] which appeared to reflect a lack of proton mobility in the ice interior. This confusion was clarified by the discovery of Lee et al.,[18−20] who showed that excess protons thermodynamically prefer to reside at the ice surface rather than in the interior. Because of this property, protons in fact collected at the surface of ice samples in the proton mobility experiments with soft-landed H_3O^+ ions over a wide temperature range,[24] while possessing high mobility in the ice sample interior to be able to reach the surface.[20,25,26] The trapping of protons at the ice surface further implies that proton migration along the ice surface does not occur as efficiently as that in the ice interior. Studies of H/D exchange reaction on ice surface indicate that for surface proton transfer a small but substantial energy barrier (∼10 kJ mol^{-1}), which is associated with proton trapping in the surface potential minimum, must be overcome.[27] Accordingly, proton transfer along the ice surface occurs by thermal activation above a certain temperature or by chemical activation of the ice surface,[17,27,28] in contrast to efficient proton transfer in the ice interior over a wide temperature range.[7−14]

Theoretical calculations using a hybrid quantum mechanics/molecular mechanics approach indicate that an excess proton is not trapped in a potential energy minimum in the ice crystal but can transfer with a small energy barrier.[29] The proton hopping along the hydrogen-bonded network of ice is coupled with the lattice geometry relaxation to facilitate sequential proton transfers in a concerted fashion.[29] An interesting question is whether proton hopping can occur in ice at extremely low temperatures, i.e., when the lattice thermal vibration is minimized and not readily available to assist in the proton transfer. The proton conductivity in ice is closely related to various ice phenomena at low temperatures, including proton order/disorder phase transitions,[30] charge distributions at the ice surface and interior,[22] and proton transfer reactions in ice.[3] However, to our best knowledge, direct evidence has not been reported as yet for the mobility of excess protons in cryogenic ice near 0 K. There are some observations that indirectly support proton mobility under these conditions.[22,31−34] For example, infrared spectra of acid-doped amorphous solid water (ASW) samples showed an intense absorption of the Zundel continuum, which could be related to concerted proton transfers in the lattice.[31,33,34] The surface voltage measurement of ice films with adsorbed acids showed that the positive protonic charge was spread over a

Received: December 8, 2018
Revised: January 11, 2019
Published: January 14, 2019

DOI: 10.1021/acs.jpcc.8b11829
J. Phys. Chem. C 2019, 123, 3657−3663

considerable depth from the surface, which was possibly due to fluctuating excess protons near the ice surface.[22] Spontaneous dissociation of halogenated acetic acids has been observed in ASW at 10−140 K, indicating efficient proton injection and migration in the lattice.[31,32] Notably, although slightly different from the transport of excess protons, concerted motion of multiple protons has been observed in *pure* ice samples at 5 K.[15] Quasi-elastic neutron scattering (QENS) studies of pure crystalline ice (CI) samples in Ih and Ic phases have shown that proton dynamics do not freeze out even at 5 K, which indicates a simultaneous movement of several protons by quantum tunneling in proton-ordered hexagonal loops that are present in a macroscopic, proton-disordered ice crystal.[15]

The present study aims to explore the possibility of quantum tunneling of excess protons in ice at very low temperatures. An experimental scheme was devised to measure proton transport from a proton donor to an acceptor species that was placed at controlled separation distances within an ice sample. For CI, however, such a sample structure could not be constructed because excess protons in the ice sample interior migrate spontaneously to the surface during crystallization of the sample at high temperatures,[19,20,25] as mentioned above. For this reason, the structure was constructed with an ASW film by vapor deposition in a vacuum at a sufficiently low temperature to suppress efficient diffusion of excess protons. The measurement of proton transport in this sample gave information about proton mobility in ASW, most likely in the microscopic ice crystallites present in the sample. Nevertheless, the results may prove to be a useful guide for judging proton mobility in CI as well.

2. EXPERIMENTAL SECTION

The experiment was conducted in an ultrahigh vacuum (UHV) chamber, which was equipped with a quadrupole mass spectrometer (QMS; Extrel, MAX-500HT) and a Fourier transform infrared (FTIR) spectrometer (Bruker, Vertex 70).[35,36] A Pt(111) single crystal was cooled by a closed-cycle He cryostat (Sumitomo Heavy Industries, CH-204N) and heated by bombardment of 2 keV electrons from a homemade electron gun attached behind the crystal. The sample could be cooled to ∼10 K and heated above 1200 K. The lowest achievable temperature (∼10 K) was estimated from an extrapolation of the sample heating/cooling rates because this temperature was below the range (>15 K) of the attached N-type thermocouple. The Pt(111) crystal substrate (surface atomic density = 1.5×10^{19} Pt atoms m^{-2}) was cleaned by 2 keV Ar^+ ion sputtering and heating to 1200 K. The ASW films were grown on the Pt(111) substrate maintained at 80 K at a growth rate <0.2 monolayer (ML; 1 ML = 1.1×10^{19} water molecules m^{-2}) per second by backfilling the chamber with water vapor. Water self-diffusion is prohibited at this temperature.[37] Hydrogen chloride (HCl, ≥99% purity) and ammonia (NH_3, 99.999% purity) gases were deposited onto the sample surface by using separate tube dosers and leak values. The background partial pressure of these gases was kept below 4×10^{-8} Pa during deposition to prevent the contamination of the chamber wall.

Temperature-programmed desorption (TPD) experiments were performed to estimate the thickness of the ASW film as well as the amounts of HCl and NH_3 in the samples. The film thickness was estimated by comparing the intensities of water desorption signal (m/z 18) produced from the ASW film and the water monolayer on Pt(111). Similarly, HCl and NH_3 coverages were determined by comparing their desorption intensities to that of their known desorption features on Pt(111).[38−40]

Reflection−absorption infrared spectroscopy (RAIRS) was used to measure the amounts of hydronium ions, ammonium ions, and NH_3 molecules in the samples. Incident p-polarized IR light was reflected from the sample at a grazing angle (85°) and entered an external mercury−cadmium−telluride detector. Dry N_2 gas was used to purge H_2O and CO_2 gases from the beam path. All spectra were recorded at ∼10 K to maintain constant baseline intensities and were averaged for 1024 scans with a spectral resolution of 4 cm^{-1}.

3. RESULTS

The transport of excess protons was studied by preparing an ASW sample with a four stacked-layer structure, as shown in Figure 1. The sample consisted of a bottom ASW film grown on a Pt(111) surface, an adsorbed HCl (proton donor) layer, ASW spacer film, and adsorbed NH_3 (proton donor) layer. The sample preparation procedure and the RAIR spectra recorded at each preparation stage are shown in Figure 1. First, a bottom ASW layer was grown on a Pt(111) substrate for a thickness of ∼70 ML (Figure 1I). The corresponding vibrational spectrum showed characteristic features of a pure ASW film (Figure 1a),[41,42] which include a strong O−H stretching band (∼3400 cm^{-1}) and H−O−H bending vibration (1660 cm^{-1}). An intermolecular libration band (∼900 cm^{-1}) appeared outside the spectral display range.[43,44]

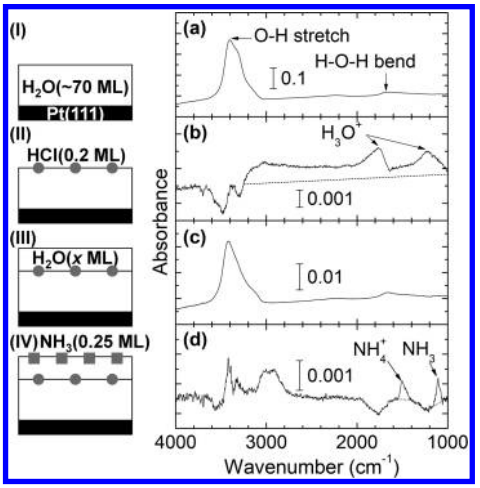

Figure 1. (I−IV) Schematics of preparation stages of NH_3(0.25 ML)/ASW(x ML)/HCl(0.2 ML)/ASW(∼70 ML) film ("HCl-sandwich" structure) on a Pt(111) substrate. The sequence of growth from the bottom to top layer is (I) ASW substrate film, (II) HCl adsorbate, (III) ASW spacer film, and (IV) NH_3 adsorbate. Steps I−III were performed at 80 K for all samples. Ammonia adsorption (step IV) was performed at either ∼10 or 80 K. (a−d) Difference RAIR spectra before and after the corresponding steps. The ASW spacer layer in (c) had a thickness of 7 ML. The dotted line in spectrum (b) is the spectral baseline drawn to indicate the Zundel continuum absorption.

Next, HCl was adsorbed for 0.2 ML on the ASW film surface (Figure 1II). The two bands at 1225 and 1760 cm^{-1} were discernible in the difference spectrum (Figure 1b), which corresponded to symmetric and asymmetric bending of H_3O^+, respectively.[45] The Zundel continuum absorption due to excess protons also appeared in the region of 1000−3000 cm^{-1},[31,46] as marked by the dotted line. These features,

DOI: 10.1021/acs.jpcc.8b11829
J. Phys. Chem. C 2019, 123, 3657−3663

together with the absent H−Cl stretch band (~2500 cm^{-1}) of molecular HCl with hydrogen bonding to the surface, confirmed the complete dissociation of HCl into excess protons and chloride ions at 80 K.[47−50] The negative absorption near 3400 cm^{-1} was consistent with the conversion of a certain portion of water molecules into hydronium ions. Subsequently, on this HCl adsorbate layer, an ASW film was overlaid with a controlled thickness (Figure 1III), which defined the distance between the proton donor (HCl) and acceptor (NH_3). The difference spectrum of this ASW spacer layer (Figure 1c) was nearly identical to that in Figure 1a.

Lastly, NH_3 molecules were adsorbed for 0.25 ML on top of the ASW spacer film (Figure 1IV). The NH_3 adsorption was performed at either ~10 or 80 K. This temperature defines the temperature of proton transfer through ASW from HCl to NH_3. As presented in Figure 1d, NH_3 adsorption produced various changes in the spectrum. The symmetric bend (ν_2) of NH_3 at 1100 cm^{-1} appeared as a result of ammonia adsorption.[21,45] The asymmetric bend (ν_4) of NH_4^+ at 1480 cm^{-1} could be attributed to proton transfer to NH_3. The negative absorptions at 1760 and 1210 cm^{-1} indicated a decreased population of hydronium ions because of proton transfer. The complex features at 2800−3600 cm^{-1} indicated changes in the N−H stretch intensity of NH_3 and the O−H stretch intensity of water. All these features indicated the occurrence of acid−base reaction 1 by transport of excess protons through the ASW spacer film

$$H_3O^+(b) + NH_3(s) \rightarrow H_2O(b) + NH_4^+(s) \quad (1)$$

where (s) and (b) designate surface and bulk species, respectively. It was observed that the reaction instantaneously occurred following the adsorption of ammonia onto the ASW surface. No further increase in the reaction yield was observed after a time delay of RAIRS measurement up to 1 h.

The present sample structure ("HCl-sandwich" structure) was chosen to assess proton transfer because it had two advantages over the "NH_3-sandwich" structure with the reversed positions of HCl and NH_3, which was used in the previous studies.[21] The first advantage is that the initial amount of excess protons in the sample can be accurately determined for the HCl-sandwich sample because of complete dissociation of HCl inside an ASW film at the temperature (80 K) of the sample preparation.[47−50] In contrast, when the NH_3-sandwich film is used, the adsorption of HCl onto the ASW film surface needs to be performed in the final stage of sample formation at the temperature of proton transfer (10 or 80 K). However, the degree of HCl dissociation on the ASW surface at 10 K is unknown. Second, the sticking coefficient of water molecules on hydronium ions present on the ASW surface is close to unity. This makes an ASW spacer layer grow on them with near uniform thickness. On the other hand, the low sticking probability (~0.14 at ~90 K) of water molecules on NH_3 adsorbates hampers the growth of ASW spacer layer with a uniform thickness in the NH_3-sandwich sample.[21]

The proton transfer yield in reaction 1 was measured as a function of the donor−acceptor distance by changing the ASW spacer thickness. Figure 2a displays the difference spectra in the 1000−2000 cm^{-1} region measured after ammonia adsorption at 80 K, which were obtained for samples with varying thicknesses of the spacer layer. Figure 2b shows the corresponding results obtained for ammonia adsorption at ~10 K. In both cases, the features arising as a result of reaction 1, aforementioned in Figure 1d, were clearly observable. The ν_2

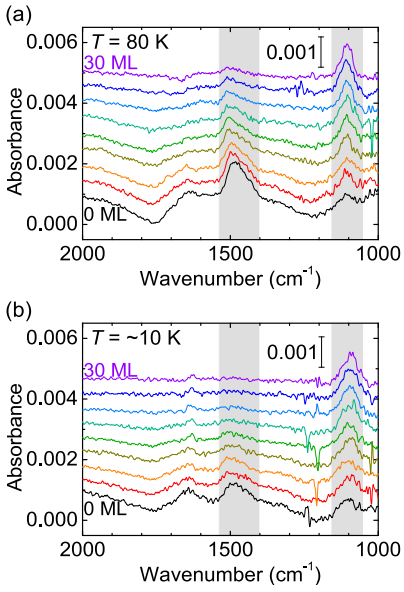

Figure 2. Difference RAIR spectra measured after ammonia adsorption for a coverage of 0.25 ML onto the surface of ASW(0−30 ML)/HCl(0.2 ML)/ASW(~70 ML)/Pt(111) samples. Ammonia adsorption was performed at temperatures (a) 80 K and (b) ~10 K. The thickness of the ASW spacer layer in the samples was 0, 2, 3, 5, 7, 10, 15, 20, and 30 ML, from the bottom to top spectra in (a) and (b). The vertical spacing between the spectra is for visual clarity. Gray shades highlight the positions of the ν_4 band of NH_4^+ (~1480 cm^{-1}) and the ν_2 band of NH_3 (~1100 cm^{-1}). Glitch peaks around 1200 cm^{-1} in several spectra can be attributed to noise that most likely originated from the mechanical vibration of a He cryostat.

band of NH_3 at ~1100 cm^{-1} and the ν_4 band of NH_4^+ at ~1480 cm^{-1} attributable to ammonia adsorption and proton transfer, respectively, were observed. At the same time, the absorbances of the symmetric (1225 cm^{-1}) and asymmetric (1760 cm^{-1}) bending vibrations of hydronium ions decreased. These changes were more pronounced when the thickness of ASW spacer was narrower and the sample temperature was higher. The weak absorption feature at ~1630 cm^{-1} could be the symmetric bending of NH_4^+.[51,52] Although this vibrational mode is IR-inactive for NH_4^+ in the gas phase, it could be IR-active for the surface-adsorbed species because of the symmetry breaking associated with hydrogen bonding to the surface. This feature could also be a visual distortion effect in the spectrum due to the depletion of H_3O^+ asymmetric bend intensity located nearby (~1760 cm^{-1}). The scissoring (asymmetric bending) mode of NH_3 could also appear in this position.

The spectrum displayed at the bottom of each series in Figures 2a and 2b corresponds to the sample without an ASW spacer film. In this sample, proton transfer occurred *along the surface* of the ASW sample between H_3O^+ and NH_3 located on the surface. The efficiency of this surface proton transfer could be estimated from the NH_4^+ band intensities of these samples, as described below. The area of the ν_4 band of NH_4^+ at ~1480 cm^{-1} was converted to NH_4^+ population with the help of a calibration experiment, which measured the ν_4 band area for a known amount (0.25 ML) of NH_4^+ produced by a stoichiometric reaction between NH_3 (0.25 ML) and HCl (in excess) on the ASW film surface. Separate calibration experiments were performed at ~10 and 80 K. Then, the efficiency of the surface proton transfer was calculated by

DOI: 10.1021/acs.jpcc.8b11829
J. Phys. Chem. C 2019, 123, 3657−3663

dividing the population of NH_4^+ with the initial population of hydronium ions on the sample surface. This quantitation procedure revealed that almost all hydronium ions that are initially present on the surface reacted with adsorbed ammonia molecules to form NH_4^+ at 80 K. This reacted portion was reduced to about 44% at 10 K, indicating that the surface proton transfer efficiency varied significantly depending on the temperature. This behavior is consistent with the fact that an excess proton is trapped in a shallow potential minimum on the ASW surface,[19,20] and its migration along the surface requires it to overcome an energy barrier of ~10 kJ mol^{-1} with the help of thermal or chemical energy,[27] as mentioned in section 1. Accordingly, a substantially large portion of excess protons was trapped in position on the ASW surface without migrating to NH_3 at ~10 K. For the present coverages of HCl (0.2 ML) and NH_3 (0.25 ML), the average distance between the proton donor and acceptor was about two water molecules. Therefore, the result indicated that 44% of excess protons could move across two water molecules at ~10 K. This surface migration of protons could be activated by local heating of the surface upon ammonia adsorption. At 80 K, thermal energy may additionally contribute to overcoming the surface diffusion barrier, which extends the proton transfer distance to significantly longer than two water molecules.

Proton transfer efficiency *through* ASW can be estimated from the results of proton transfer measurements as a function of the ASW spacer thickness. This proton transfer efficiency (η) was calculated only for the "mobile" protons in the sample. A "mobile" proton refers to an excess proton that is not permanently trapped in the potential well in its initially created position at the corresponding temperature. When both hydronium ions and ammonia molecules are placed on the surface of an ASW film, only "mobile" protons can migrate along the surface to produce NH_4^+, whereas "immobile" protons are trapped in the potential well of the surface at fixed positions. Therefore, it was considered that the population of mobile surface protons would be equal to the population of NH_4^+ ions measured in the surface proton transfer experiment in the absence of an ASW spacer film, $\theta_{\text{mobile H}^+} = \theta_{NH_4^+}(0\ \text{ML})$, where θ_A is the surface population of A species. As mentioned above, almost all excess protons present on the ASW surface were "mobile" at 80 K, but this portion decreased to about 44% at ~10 K. It was assumed that the same ratio for mobile/immobile excess protons was maintained underneath the ASW spacer layer at corresponding temperatures. This assumption was based on the rationale that thermal rearrangement of the H-bonded water structure does not easily occur at the temperature (80 K) of sample preparation.[9−11] Of course, water adsorption on the surface may perturb the proton trapping structures and may convert some of these immobile protons to mobile protons underneath the ASW spacer film. This effect, however, appeared to be insignificant in the spectra shown in Figure 2, which showed a smooth decrease, rather than a discontinuous increase, in the ammonium formation yield as a thin ASW layer was overlaid on the surface hydronium ions. Based on these considerations, the proton transfer efficiency through ASW across the film thickness of x could be determined by the equation

$$\eta(x) = \frac{\theta_{NH_4^+}(x)}{\theta_{\text{mobile H}^+}} = \frac{\theta_{NH_4^+}(x)}{\theta_{NH_4^+}(0\ \text{ML})}$$

The $\eta(x)$ curves at ~10 and 80 K estimated from the data set presented in Figure 2 are plotted in Figure 3. The value of $\eta(x)$

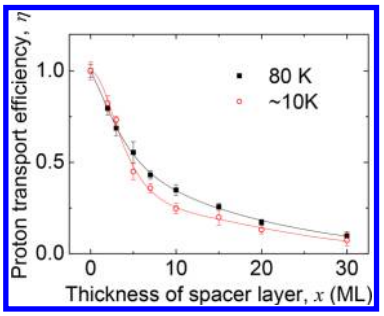

Figure 3. Proton transfer efficiency versus the thickness of ASW spacer layer measured at 80 K (black solid squares) and ~10 K (red open circles). The normalized $\eta(x)$ curves represent the transport efficiencies of "mobile" excess protons in the sample. The error bars correspond to the uncertainty for the quantitation of proton donor and acceptor species through RAIRS measurement.

decreased from unity at x = 0 to below 0.1 at x = 30 ML at both temperatures. The average distance of proton transfer through ASW was calculated by integrating $\eta(x)$ over x. The average proton-transfer distance calculated in this way was $\langle x \rangle$ = 11.2 ± 1.1 ML at 80 K and 9.4 ± 1.4 ML at ~10 K. In the case of an "NH_3-sandwich" sample, a correction for the nonuniform thickness of ASW spacer layer has previously been implemented for a more realistic estimation of $\langle x \rangle$,[21] but this correction had little impact (±1 ML) on improving the $\langle x \rangle$ value of the present samples. Thus, proton transfer distance was considered basically equal to the thickness of the spacer layer.

4. DISCUSSION

When the present samples were prepared by the growth of an ASW spacer layer over the hydronium ions (stage 1-III) at 80 K, it was assumed that the hydroniums stayed in position without upward diffusion. However, the hydronium ions could undergo thermal diffusion and accumulate at the surface of a growing ASW film at high temperature because of their thermodynamic affinity for the ice surface.[19,20,26] For this reason, the possibility of upward diffusion of hydronium ions at 80 K was worth investigating. The necessary information could be obtained from the measurement of the surface voltages of HCl-doped ASW films, as described by Lee et al.[22] An analysis of the changes in the film voltage with the growth of the ASW overlayer on the HCl-adsorbed ASW surface at 95 K (Figure 5 in ref 22) showed that the average penetration depth of excess protons into the ASW overlayer was 3.5 ML when the HCl adsorbate coverage was 0.04 ML. This penetration depth decreased with an increase in HCl coverage, probably as a result of electrostatic interactions between H^+ and Cl^- ions. Based on this reference, the upward penetration of excess protons into ASW spacer layer in the present samples was expected to be <3.5 ML because of a higher HCl content (0.2 ML) and a slightly lower temperature. Therefore, the absolute distance of proton migration in the present measurements likely had this magnitude of uncertainty (<3.5 ML). When the relative differences in the proton transfer distances at two different temperatures were assessed, this uncertainty would mostly cancel out because the same temperature (80 K) was used for the growth of the ASW spacer in all samples.

DOI: 10.1021/acs.jpcc.8b11829
J. Phys. Chem. C 2019, 123, 3657−3663

Moon et al.[21] conducted similar experiments as described in this study, except that the locations of HCl and NH_3 in the samples were reversed ("NH_3-sandwich" structure), and reported that the average proton migration distance, $\langle x \rangle$, was 11.3 ML in ASW films at 90 K. The two studies show good agreement of the $\langle x \rangle$ values (11.3 and 11.2 ML) at similar temperatures (80 and 90 K), which supports the validity of the experimental approaches. The upward migration of excess protons did not occur in the experiments conducted by Moon et al.[21] because NH_3 was located in the sandwich layer and hydronium ions were at the surface of the samples. Therefore, the agreement in $\langle x \rangle$ values implied that the upward migration of excess protons in the present samples was not extensive.

In the discussion above, two different quantities relating to proton transport ranges have been mentioned, and it is worthwhile clarifying the differences between them. The proton transport distance (x) measured in this study and by Moon et al.[21] is the actual migration distance of excess protons from the proton donor to the acceptor species. This proton transport process occurs irreversibly in one direction. On the other hand, the penetration depth of excess protons into an ASW film discussed for the film voltage measurement[22] corresponds to the distance of positive charge displacement from the initial injection position of hydronium ions in the sample, in the absence of proton acceptor species. The excess protons in this case may commute back and forth reversibly while residing near the location of the initial hydronium injection. The latter may represent the time-averaged position of protons commuting in the solid lattice. Therefore, the former (9−11 ML at 10−80 K) is always greater than the latter (3.5 ML at 95 K).

The present study shows two notable features for proton transfer in ASW. One is that proton transfer occurs in ASW at temperatures as low as ∼10 K. The observed proton transfer distance in ASW is 9.4 ± 1.4 ML at this temperature, whereas the range of proton transfer along the ASW surface is substantially shorter (about 2 ML). Considering the possibility of local heating of the surface by ammonia adsorption, the surface proton transfer may actually be more restricted if the ammonia adsorption effect is excluded, which is consistent with the fact that surface proton transfer is an activated process.[27] At 10 K, essentially all atoms and molecules are immobilized with minimal thermal motion at the fixed lattice positions. Theoretical calculations[29] indicate that the barrier height for transport of excess proton in ice is ∼50 kJ mol^{-1} when the O−O distance of the ice crystal is fixed, and it decreases to 6 kJ mol^{-1} for the minimum-energy path with full geometry optimization, although the feasibility of such lattice distortion in cryogenic ice is questionable. These barrier heights are far too large for proton transfer to occur at 10 K. For example, the expected classical rate of proton transfer over the barrier of 6 kJ mol^{-1} is only $k \sim 5 \times 10^{-19}$ s^{-1} at 10 K with a frequency factor of 10^{13} s^{-1}. Therefore, the observed proton transfer must occur via quantum tunneling. The other feature is that the proton transfer distance is independent of the temperature, as indicated by the almost negligible difference (1.8 ± 1.8 ML) between the $\langle x \rangle$ values at 10 and 80 K. This behavior contrasts with the significantly different efficiencies of proton transfer along the surface at 10 and 80 K. If it is considered that the different proton transfer efficiencies on the surface could somehow interfere with the measurements of vertical proton transfer in the present experiment, such a small difference in the $\langle x \rangle$ values may be physically meaningless. The temperature independence again supports the quantum tunneling of excess protons. Previously, quantum tunneling phenomena of protons have been observed in experiments using pure ice crystals[15] and water nanoclusters[53] and studied by theoretical calculations.[54] In these cases, concerted tunneling of multiple protons occurs in proton-ordered rings present in ice crystals or nanoclusters without acid additives. This involves simultaneous migration of charge defects in the loop without changing the net dipole moment in the whole proton transfer structure. The present system is different from these cases in that a net charge is carried through the lattice by the transport of excess protons.

The structure of ASW films prepared at 80 K must inevitably have an incomplete hydrogen-bonding network with high density of defects. In this environment, proton tunneling may be possible only in those localized regions of the sample that have a crystalline-like structure with a well-ordered hydrogen-bond network. Abundant defects and incompletely coordinated molecules in the sample may act as permanent traps of excess protons at low temperature.[9−11] Consequently, the proton transfer efficiency decreases rapidly with an increase in the donor−acceptor separation distance. In other words, the proton transfer distance in ASW is limited by the hydrogen-bond connectivity of the lattice, which implies that the proton transfer distance may vary depending on the preparation conditions of the ASW sample. Besides, the proton transfer distance is expected to be substantially longer in a macroscopic ice crystal with low defect density.

The occurrence of proton tunneling at low temperature has useful implications for cryogenic ice chemistry. Recent studies have shown that fluoroacetic acids spontaneously dissociate in ASW at low temperature (10−140 K) with a higher yield than that in aqueous solutions at room temperature.[31,32] These phenomena have been explained in terms of the proposition that acid dissociation is driven by the configurational entropy of mobile excess protons in the ice lattice.[32] The occurrence of proton tunneling in ASW at low temperature supports this interpretation that highly mobile protons can generate a substantially large configurational entropy. Similar effects have also been suggested for the promotion of crystallization of ASW films in the presence of acids.[50] In general, it has been considered extremely difficult for chemical reactions to occur spontaneously in cryogenic ice because of the immobility of atoms and molecules as well as the lack of thermal energy to overcome the reaction activation energy. For example, in the ice environments of the outer planets of the solar system and the interstellar medium,[55,56] it has thus far been assumed that chemical reactions are driven mostly by external energy input. However, the availability of proton tunneling in cryogenic ice suggests that certain types of proton transfer reactions may be able to occur spontaneously even under these conditions, as has been observed for the dissociation of fluoroacetic acids in ice.[31,32]

5. CONCLUSIONS

In this study, the transport efficiency of excess protons in ASW was examined at the low temperatures at which only proton hopping motion was possible without thermal reorientation of water molecules. It was found that the diffusion of excess protons occurred in ASW at temperatures as low as ∼10 K. The average proton-transport distances were 9.4 ± 1.4 and 11.2 ± 1.1 ML at 10 and 80 K, respectively, through the ASW film prepared by vapor deposition at 80 K. On the other hand,

DOI: 10.1021/acs.jpcc.8b11829
J. Phys. Chem. C 2019, 123, 3657−3663

proton diffusion along the ASW surface hardly occurred at 10 K because of an activation energy barrier. The observations that proton transfer through ASW was nearly independent of the temperature and took place over a substantially longer distance than surface proton transfer indicated the quantum tunneling nature of excess protons in ASW. The observed proton transfer may occur in microscopic crystalline-like regions of the ASW samples, implying that the proton transfer distance may be much longer in an ice crystal. This study confirmed the assumption in previous studies[16,31,32,50] that excess protons are uniquely mobile species in ice at low temperatures and may contribute to various physical and chemical phenomena in these environments.

AUTHOR INFORMATION

Corresponding Author

*E-mail surfion@snu.ac.kr, Tel +82 2 875 7471, Fax +82 2 889 8156.

ORCID

Heon Kang: 0000-0002-7530-4100

Present Address

D.H.L.: Korea Polar Research Institute, 26 Songdomirae-ro, Yeonsu-gu, Incheon 21990, Republic of Korea.

Notes

The authors declare no competing financial interest.

ACKNOWLEDGMENTS

This work was supported by Korea Polar Research Institute (KOPRI) project (PE19200).

REFERENCES

(1) Fletcher, N. H. *The Chemical Physics of Ice*; Cambridge University Press: Cambridge, 1970.

(2) Petrenko, V. F.; Whitworth, R. W. *Physics of Ice*; Oxford University Press: Oxford, 1999.

(3) Kang, H. Chemistry of Ice Surfaces. Elementary Reaction Steps on Ice Studied by Reactive Ion Scattering. *Acc. Chem. Res.* **2005**, *38*, 893−900.

(4) Jaccard, C. Etude Theorique Et Experimentale Des Proprietes De La Glace. *Helv. Phys. Acta* **1959**, *32*, 89−128.

(5) Jaccard, C. Thermodynamics of Irreversible Processes Applied to Ice. *Phys. Kondens. Mater.* **1964**, *3*, 99−118.

(6) Onsager, L.; Dupuis, M. The Electrical Properties of Ice. In *Electrolytes*; Pesce, B., Ed.; Pergamon Press: Oxford, 1962; pp 27−46.

(7) Eigen, M.; De Maeyer, L. Self-Dissociation and Protonic Charge Transport in Water and Ice. *Proc. R. Soc. London, Ser. A* **1958**, *247*, 505−533.

(8) Eigen, M. Proton Transfer, Acid-base Catalysis, and Enzymatic Hydrolysis. Part I: Elementary processes. *Angew. Chem., Int. Ed. Engl.* **1964**, *3*, 1−19.

(9) Collier, W. B.; Ritzhaupt, G.; Devlin, J. P. Spectroscopically Evaluated Rates and Energies for Proton-Transfer and Bjerrum Defect Migration in Cubic Ice. *J. Phys. Chem.* **1984**, *88*, 363−368.

(10) Wooldridge, P. J.; Devlin, J. P. Proton Trapping and Defect Energetics in Ice from FT-IR Monitoring of Photoinduced Isotopic Exchange of Isolated D_2O. *J. Chem. Phys.* **1988**, *88*, 3086−3091.

(11) Fisher, M.; Devlin, J. P. Defect Activity in Amorphous Ice from Isotopic Exchange Data: Insight into the Glass Transition. *J. Phys. Chem.* **1995**, *99*, 11584−11590.

(12) Uritski, A.; Presiado, I.; Huppert, D. Indication of a Very Large Proton Diffusion in Ice I_h. *J. Phys. Chem. C* **2008**, *112*, 11991−12002.

(13) Uritski, A.; Presiado, I.; Erez, Y.; Gepshtein, R.; Huppert, D. Temperature Dependence of Proton Diffusion in I_h Ice. *J. Phys. Chem. C* **2009**, *113*, 10285−10296.

(14) Presiado, I.; Lal, J.; Mamontov, E.; Kolesnikov, A. I.; Huppert, D. Fast Proton Hopping Detection in Ice I_h by Quasi-Elastic Neutron Scattering. *J. Phys. Chem. C* **2011**, *115*, 10245−10251.

(15) Bove, L. E.; Klotz, S.; Paciaroni, A.; Sacchetti, F. Anomalous Proton Dynamics in Ice at Low Temperatures. *Phys. Rev. Lett.* **2009**, *103*, 165901.

(16) Park, S. C.; Moon, E. S.; Kang, H. Some Fundamental Properties and Reactions of Ice Surfaces at Low Temperatures. *Phys. Chem. Chem. Phys.* **2010**, *12*, 12000−12011.

(17) Park, S. C.; Jung, K. H.; Kang, H. H/D Isotopic Exchange between Water Molecules at Ice Surfaces. *J. Chem. Phys.* **2004**, *121*, 2765−2774.

(18) Lee, C. W.; Lee, P. R.; Kang, H. Protons at Ice Surfaces. *Angew. Chem., Int. Ed.* **2006**, *45*, 5529−5533.

(19) Lee, C. W.; Lee, P. R.; Kim, Y. K.; Kang, H. Mechanistic Study of Proton Transfer and H/D Exchange in Ice Films at Low Temperatures (100−140 K). *J. Chem. Phys.* **2007**, *127*, 084701.

(20) Moon, E. S.; Lee, C. W.; Kang, H. Proton Mobility in Thin Ice Films: A Revisit. *Phys. Chem. Chem. Phys.* **2008**, *10*, 4814−4816.

(21) Moon, E. S.; Kim, Y.; Shin, S.; Kang, H. Asymmetric Transport Efficiencies of Positive and Negative Ion Defects in Amorphous Ice. *Phys. Rev. Lett.* **2012**, *108*, 226103.

(22) Lee, D. H.; Bang, J.; Kang, H. Surface Charge Layer of Amorphous Solid Water with Adsorbed Acid or Base: Asymmetric Depth Distributions of H^+ and OH^- Ions. *J. Phys. Chem. C* **2016**, *120*, 12051−12058.

(23) Devlin, J. P. Relating the Current Science of Ion-Defect Behavior in Ice to a Plausible Mechanism for Directional Charge Transfer During Ice Particle Collisions. *Phys. Chem. Chem. Phys.* **2011**, *13*, 19707−19713.

(24) Cowin, J. P.; Tsekouras, A. A.; Iedema, M. J.; Wu, K.; Ellison, G. B. Immobility of Protons in Ice from 30 to 190 K. *Nature* **1999**, *398*, 405−407.

(25) Lilach, Y.; Iedema, M. J.; Cowin, J. P. Proton Segregation on a Growing Ice Interface. *Surf. Sci.* **2008**, *602*, 2886−2893.

(26) Park, E.; Lee, D. H.; Kim, S.; Kang, H. Transport and Surface Accumulation of Hydroniums and Chlorides in an Ice Film. A High Temperature (140−180 K) Study. *J. Phys. Chem. C* **2012**, *116*, 21828−21835.

(27) Moon, E. S.; Yoon, J.; Kang, H. Energy Barrier of Proton Transfer at Ice Surfaces. *J. Chem. Phys.* **2010**, *133*, 044709.

(28) Park, K.; Lin, W.; Paesani, F. Fast and Slow Proton Transfer in Ice: The Role of the Quasi-Liquid Layer and Hydrogen-Bond Network. *J. Phys. Chem. B* **2014**, *118*, 8081−8089.

(29) Kobayashi, C.; Saito, S. J.; Ohmine, I. Mechanism of Fast Proton Transfer in Ice: Potential Energy Surface and Reaction Coordinate Analyses. *J. Chem. Phys.* **2000**, *113*, 9090−9100.

(30) Castro Neto, A. H.; Pujol, P.; Fradkin, E. Ice: A Strongly Correlated Proton System. *Phys. Rev. B: Condens. Matter Mater. Phys.* **2006**, *74*, 024302.

(31) Shin, S.; Park, Y.; Kim, Y.; Kang, H. Dissociation of Trifluoroacetic Acid in Amorphous Solid Water: Charge-Delocalized Hydroniums and Zundel Continuum Absorption. *J. Phys. Chem. C* **2017**, *121*, 12842−12848.

(32) Park, Y.; Shin, S.; Kang, H. Entropy-Driven Spontaneous Reaction in Cryogenic Ice: Dissociation of Fluoroacetic Acids. *J. Phys. Chem. Lett.* **2018**, *9*, 4282−4286.

(33) Ayotte, P.; Hébert, M.; Marchand, P. Why Is Hydrofluoric Acid a Weak Acid? *J. Chem. Phys.* **2005**, *123*, 184501.

(34) Marchand, P.; Marcotte, G.; Ayotte, P. Spectroscopic Study of HNO_3 Dissociation on Ice. *J. Phys. Chem. A* **2012**, *116*, 12112−12122.

(35) Kang, H.; Shin, S.; Park, Y.; Kang, H. Electric Field Effect on Condensed-Phase Molecular Systems. III. The Origin of the Field-Induced Change in the Vibrational Frequency of Adsorbed CO on Pt(111). *J. Phys. Chem. C* **2016**, *120*, 17579−17587.

(36) Park, Y.; Kang, H.; Kang, H. Brute Force Orientation of Matrix-Isolated Molecules: Reversible Reorientation of Formaldehyde in an

DOI: 10.1021/acs.jpcc.8b11829
J. Phys. Chem. C 2019, 123, 3657−3663

Argon Matrix toward Perfect Alignment. *Angew. Chem., Int. Ed.* **2017**, *56*, 1046−1049.
(37) Livingston, F. E.; Smith, J. A.; George, S. M. General Trends for Bulk Diffusion in Ice and Surface Diffusion on Ice. *J. Phys. Chem. A* **2002**, *106*, 6309−6318.
(38) Daschbach, J. L.; Kim, J.; Ayotte, P.; Smith, R. S.; Kay, B. D. Adsorption and Desorption of HCl on Pt(111). *J. Phys. Chem. B* **2005**, *109*, 15506−15514.
(39) Fisher, G. B. The Electronic Structure of Two Forms of Molecular Ammonia Adsorbed on Pt(111). *Chem. Phys. Lett.* **1981**, *79*, 452−458.
(40) Gland, J. L.; Kollin, E. B. Ammonia Adsorption on the Pt(111) and Pt(S)-6(111)×(111) Surfaces. *Surf. Sci.* **1981**, *104*, 478−490.
(41) Cholette, F.; Zubkov, T.; Smith, R. S.; Dohnalek, Z.; Kay, B. D.; Ayotte, P. Infrared Spectroscopy and Optical Constants of Porous Amorphous Solid Water. *J. Phys. Chem. B* **2009**, *113*, 4131−4140.
(42) Smith, R. S.; Matthiesen, J.; Knox, J.; Kay, B. D. Crystallization Kinetics and Excess Free Energy of H_2O and D_2O Nanoscale Films of Amorphous Solid Water. *J. Phys. Chem. A* **2011**, *115*, 5908−5917.
(43) Hagen, W.; Tielens, A. G. G. M. The Librational Region in the Spectrum of Amorphous Solid Water and Ice I_c between 10 and 140 K. *Spectrochim. Acta, Part A* **1982**, *38*, 1089−1094.
(44) Severson, M. W.; Devlin, J. P.; Buch, V. Librational Modes of Ice. I. *J. Chem. Phys.* **2003**, *119*, 4449−4457.
(45) Pursell, C. J.; Zaidi, M.; Thompson, A.; Fraser-Gaston, C.; Vela, E. Acid-Base Chemistry on Crystalline Ice: HCl + NH_3. *J. Phys. Chem. A* **2000**, *104*, 552−556.
(46) Dahms, F.; Costard, R.; Pines, E.; Fingerhut, B. P.; Nibbering, E. T.; Elsaesser, T. The Hydrated Excess Proton in the Zundel Cation $H_5O_2^+$: The Role of Ultrafast Solvent Fluctuations. *Angew. Chem., Int. Ed.* **2016**, *55*, 10600−10605.
(47) Devlin, J. P.; Uras, N.; Sadlej, J.; Buch, V. Discrete Stages in the Solvation and Ionization of Hydrogen Chloride Adsorbed on Ice Particles. *Nature* **2002**, *417*, 269−271.
(48) Parent, P.; Lasne, J.; Marcotte, G.; Laffon, C. HCl Adsorption on Ice at Low Temperature: A Combined X-Ray Absorption, Photoemission and Infrared Study. *Phys. Chem. Chem. Phys.* **2011**, *13*, 7142−7148.
(49) Ayotte, P.; Marchand, P.; Daschbach, J. L.; Smith, R. S.; Kay, B. D. HCl Adsorption and Ionization on Amorphous and Crystalline H_2O Films Below 50 K. *J. Phys. Chem. A* **2011**, *115*, 6002−6014.
(50) Lee, D. H.; Kang, H. Acid-Promoted Crystallization of Amorphous Solid Water. *J. Phys. Chem. C* **2018**, *122*, 24164−24170.
(51) Martin, J. M. L.; Lee, T. J. Accurate Ab Initio Quartic Force Field and Vibrational Frequencies of the NH_4^+ Ion and Its Deuterated Forms. *Chem. Phys. Lett.* **1996**, *258*, 129−135.
(52) Jacox, M. E.; Thompson, W. E. Infrared Spectrum of the NH_4-d_n^+ Cation Trapped in Solid Neon. *Phys. Chem. Chem. Phys.* **2005**, *7*, 768−775.
(53) Meng, X.; Guo, J.; Peng, J.; Chen, J.; Wang, Z.; Shi, J.-R.; Li, X.-Z.; Wang, E.-G.; Jiang, Y. Direct Visualization of Concerted Proton Tunnelling in a Water Nanocluster. *Nat. Phys.* **2015**, *11*, 235−239.
(54) Drechsel-Grau, C.; Marx, D. Collective Proton Transfer in Ordinary Ice: Local Environments, Temperature Dependence and Deuteration Effects. *Phys. Chem. Chem. Phys.* **2017**, *19*, 2623−2635.
(55) Greenberg, J. M. Cosmic Dust and Our Origins. *Surf. Sci.* **2002**, *500*, 793−822.
(56) Watanabe, N.; Kouchi, A. Ice Surface Reactions: A Key to Chemical Evolution in Space. *Prog. Surf. Sci.* **2008**, *83*, 439−489.

DOI: 10.1021/acs.jpcc.8b11829
J. Phys. Chem. C 2019, 123, 3657−3663